

www.acsabm.org Article

Green Synthesis of Polycyclodextrin/Drug Inclusion Complex Nanofibrous Hydrogels: pH-Dependent Release of Acyclovir

Asli Celebioglu* and Tamer Uyar*



Cite This: ACS Appl. Bio Mater. 2023, 6, 3798-3809



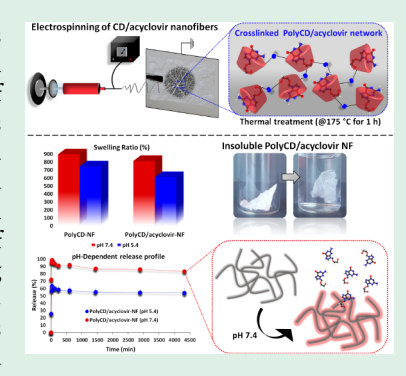
ACCESS I

Metrics & More

Article Recommendations

Supporting Information

ABSTRACT: The development of an approach or a material for wound healing treatments has drawn a lot of attention for decades and has been an important portion of the research in the medical industry. Especially, there is growing interest and demand for the generation of wound care products using eco-friendly conditions. Electrospinning is one of these methods that enables the production of nanofibrous materials with attractive properties for wound healing under mild conditions and by using sustainable sources. In this study, starch-derived cyclodextrin (hydroxypropyl-β-cyclodextrin (HPβCD)) was used both for forming an inclusion complex (IC) with acyclovir, a well-known antiviral drug, and for electrospinning of free-standing nanofibers. The nanofibers were produced in an aqueous system, without using a carrier polymer matrix and toxic solvent/chemical. The ultimate HPβCD/acyclovir-IC nanofibers were thermally cross-linked by using citric acid, listed in the generally regarded as safe (GRAS) category by the US Food and Drug Administration (FDA). The cross-linked HPβCD/acyclovir-IC nanofibers displayed stability in aqueous medium. The hydrogel-



forming feature of nanofibers was confirmed with their high swelling profile in water in the range of \sim 610–810%. Cellulose acetate (CA)/acyclovir nanofibers were also produced as the control sample. Due to inclusion complexation with HP β CD, the solubility of acyclovir was improved, so cross-linked HP β CD/acyclovir-IC nanofibrous hydrogels displayed a better release performance compared to CA/acyclovir nanofibers. Here, a pH-dependent release profile was obtained (pH 5.4 and pH 7.4) besides their attractive swelling features. Therefore, the cross-linked HP β CD/acyclovir-IC nanofibrous hydrogel can be a promising candidate as a wound healing dressing for the administration of antiviral drugs by holding the unique properties of CD and electrospun nanofibers.

KEYWORDS: cyclodextrin, electrospinning, hydrogel, acyclovir, pH-dependent release, wound dressing

1. INTRODUCTION

Skin is the largest organ in humans and plays the role of a barrier to protect the body from the entrance of exterior pathogens, to reduce fluid loss, and against temperature/chemicals. Any discontinuity occurring at the wound spot of the skin would create a pathway for undesired elements to enter the human body. 1-4 Therefore, disruption happening at the anatomic structure of the skin originating from the wound is the main problem and needs rapid healing. Wounds can be classified into subdivisions such as chronic or acute, internal or external, penetrating or nonpenetrating, open or closed, etc. based on their depth, reason, sites, and duration.⁵ Wound treatments occupy a huge commercial share in the annual market, with \$15 billion being dedicated to wound care products and \$12 billion to wound scar therapy.3 Currently, different types of wound dressing substrates are available in the market including foams, hydrogels, hydrocolloids, hydrofibers, films/strips, etc. The crucial requirements expected from the wound care materials can be listed as mechanical integrity, porosity, air/vapor permeability, absorption of exudate, and cell proliferation.⁶

The electrohydrodynamic technique of electrospinning has paved the way for a widespread research area due to its potential for large-scale development of biomaterials. ^{1-3,7} A highly porous

fibrous structure, large surface area-to-volume ratio, encapsulation capability, and lightweight and flexible features of electrospun nanofibers are favorable qualifications for biomedical applications.^{8,9} These unique properties make electrospun nanofibers particularly promising candidates for wound treatment by mimicking the composite functions and fibrous structure of the extracellular matrix (ECM) which plays a vital role in the wound healing process through cell differentiation and proliferation.^{1,5} The wound healing potential of nanofibers can be further improved by incorporation of active ingredients such as drugs, proteins, essential oils, bioactive molecules/nanoparticles, etc.⁵

Natural and synthetic biopolymers have been widely studied for the development of wound healing dressings from electrospun nanofibers due to their intrinsic biodegradability and biocompatibility. ^{5,10} Gelatin, ¹¹ chitosan, ¹² silk fibroin, ¹³ algi-

Received: June 21, 2023 Accepted: August 8, 2023 Published: August 21, 2023





ACS Applied Bio Materials www.acsabm.org Article

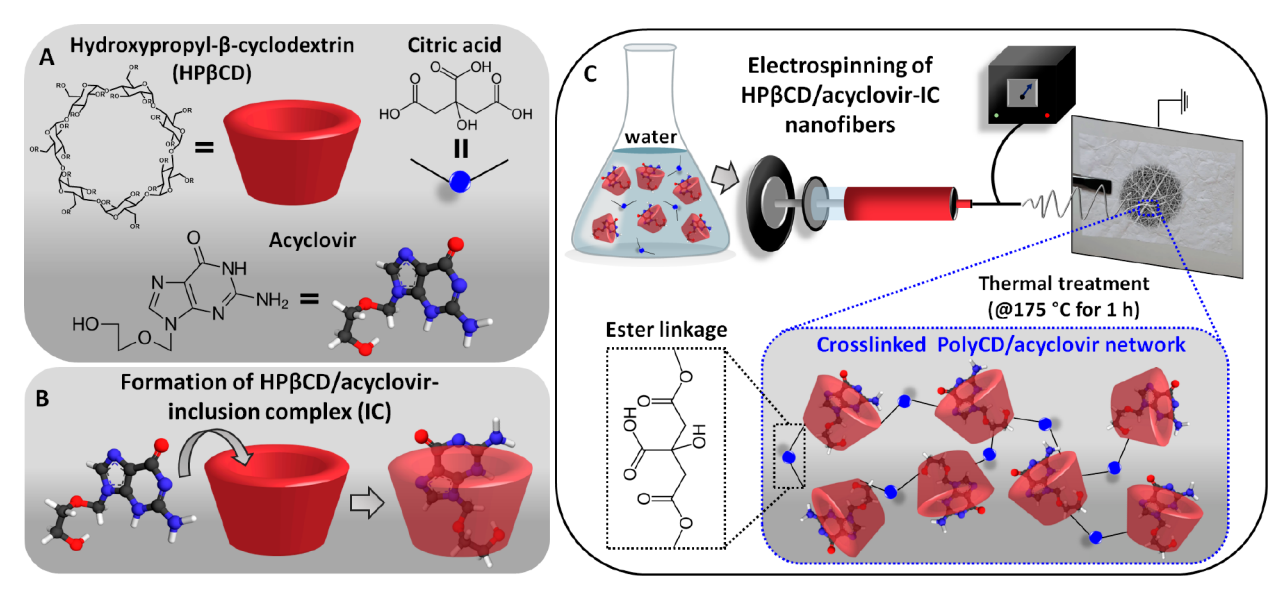


Figure 1. Schematic illustration of the sample content and preparation. (A) The chemical structure of HP β CD, citric acid, and acyclovir. The schematic representation of (B) HP β CD/acyclovir-IC formation and (C) the electrospinning and cross-linking of HP β CD/acyclovir-IC (PolyCD/acyclovir) nanofibers.

nate, 14 collagen, 15 cellulose, 16 cellulose acetate, 17 and hyaluronic acid¹⁸ are the most commonly used natural biopolymer types for the generation of nanofibers. Even though these biopolymers ensure rather good biocompatibility, biodegradability, low/no toxicity, immunogenicity, antigenicity, and low cost, they can have trouble with mechanical properties and processing due to their complex chemical structures.³ Therefore, natural biopolymers have been generally electrospun into nanofibers in a company with other polymers such as poly(ethylene oxide) (PEO), 12 poly(vinyl alcohol) (PVA), 14 polycaprolactone (PCL), 11 etc. to ensure efficient nanofiber formation. On the other hand, the use of synthetic biopolymers like PCL, 19 poly(lactic acid) (PLA), 20 poly(lactic-co-glycolic acid) (PLGA),²¹ poly(3-hydroxybutyrate-co-3-hydroxyvalerate) (PHVB),²² etc. has led to the production of wound healing materials with better mechanical properties and higher stability against environmental conditions. However, the slow biodegradation rate, lower cell affinity, and higher cost compared to natural biopolymers can be listed as the drawbacks of these synthetic biopolymers.³

As mentioned above, the electrospun nanofibers have been functionalized with different active agents to attain a proper wound healing platform. In the case of electrospinning of both natural and synthetic biopolymers, organic solvents and/or additional toxic chemicals have been used to dissolve the polymers and the active ingredients completely, and this is required to prepare an appropriate electrospinning solution.²³ The use of undesirable solvents or chemicals can be considered a major issue from the point of view of biocompatibility of the ultimate materials and environmental aspects. Therefore, there is still a huge demand for the generation of wound healing dressings using more reasonable components and eco-friendly conditions. At this point, cyclodextrins (CDs), the starchderived cyclic oligosaccharides, can be a part of the solution thanks to their nontoxic and natural properties. CDs are wellknown for their unique molecular structure, which has a donut shape with a relatively hydrophobic cavity. Due to their hydrophobic cavity, CDs can form inclusion complexes (ICs) with a variety of compounds including drugs, essential oils,

bioactive agents, etc., and this can provide enhanced aqueous solubility, bioavailability, and stability for all these active ingredients. $^{24-26}$

In the literature, it is possible to see studies in which CD-ICs of different bioactive agents (curcumin and citral) or drugs (benzocaine and naproxen) were incorporated into polymeric nanofibers for the purpose of wound care applications. 27-31 In these studies, the main goal for the integration of CD systems within the nanofiber matrix is to benefit from the solubility enhancement for poorly water-soluble compounds supplied by inclusion complexation. As was shown earlier by the Uyar research group, it is also possible to generate free-standing nanofibers from CD or CD-IC without using a carrier polymeric matrix.^{32–35} By this approach, there is no need for an organic solvent or toxic chemical to dissolve the components since electrospinning of CD-based systems is performed in water. Here, inclusion complexation ensures the dissolving of active compounds in water and therefore their amorphous distribution within the nanofibrous matrix. ^{32–35} However, CD-IC nanofibers are soluble in water and, thus, particularly proper for fastdisintegrating delivery systems. In other words, they need to be rendered into the insoluble state to obtain nanofibers that can show stability in liquid environments and display a long-term release profile that is better for wound healing treatment.

In the previous studies of the Uyar research group, the cross-linked polycyclodextrin (PolyCD) nanofibers have been generated for the filtration applications using different cross-linking agents (butanetetracarboxylic acid and epichlorohydrin). However, to the best our knowledge, the electrospinning of CD-IC nanofibers having insoluble cross-linked network structure has not yet been reported. In this study, acyclovir was chosen as the active compound for the functionalization of cross-linked CD nanofibers. Acyclovir (9-(2-hydroxyethoxymethyl)guanine) is an effective antiviral drug used for the treatment of herpes simplex virus (HSV-1/2) and varicella zoster. The administration dosage form of acyclovir includes tablets, cream, ointment, injection, and eye drops. However, the therapeutic potential of acyclovir is diminished because of its limited water solubility, low bioavailability, and

low membrane permeability. ^{39,40} On the other hand, there has been a notable effort to improve the therapeutic efficiency of this drug by improving its poor physicochemical properties using different approaches such as microemulsions, hydrogels, liposomes, nanoparticles, and CDs. ⁴⁰ Even in one of the related studies reported by Demirci et al., the cross-linked CD particles of acyclovir were formed to provide a sustained release with respectable blood compatibility. ⁴¹

In our previous study, the polymer-free CD-IC nanofibers of acyclovir were successfully produced using highly water-soluble hydroxypropyl- β -cyclodextrin (HP β CD) for the purpose of fastdisintegrating oral delivery systems. 42 The potential of acyclovirincorporated polymeric nanofibers has also been reported for HSV-2 treatments⁴³ and ocular⁴⁴ and topical delivery⁴⁵ using PLGA, PCL, and polyvinylpyrrolidone (PVP) polymers. In one of the recent studies, Kazsoki et al. showed the potential of core/ shell nanofibers of PVA/PVP for the herpes labialis treatment of acyclovir as a nanofibrous patch. 46 In this related study, HP β CD was used to enhance the solubility of acyclovir and hypromellose to retard the dissolution and therefore the initial burst release profile of ultimate nanofibers. The cross-linked and selfstanding HPβCD/acyclovir-IC nanofibers might be an emerging administration type for the topical treatment of the wound spots of cold sores, zosters, and chicken pox. Moreover, the high swelling property of this nanofiber enables the formation of nanofibrous hydrogels in the aqueous environment that is pretty attractive for the treatment of wounds. Therefore, this approach might be a reasonable alternative to the conventional dosage formulations of acyclovir creams or hydrocolloid-based patches. For this, the polymer-free HP β CD/acyclovir-IC nanofibers were produced by the incorporation of a cross-linking agent: citric acid which is listed in the generally regarded as safe (GRAS) category by the US Food and Drug Administration (FDA) due to its environmental friendliness and biodegradability. 47 The ultimate insoluble nanofibers were obtained upon postthermal treatment (Figure 1). The control nanofibers were produced using a popular biopolymer of cellulose acetate which is frequently used in biomedical applications particularly due its high water uptake property. The further characterization of these nanofibrous systems was performed to reveal their structural properties and release profiles.

2. EXPERIMENTAL SECTION

2.1. Materials. Hydroxypropyl- β -cyclodextrin (HP β CD) (Cavasol W7 HP, DS: ~0.9) was kindly presented by Wacker Chemie AG (USA). Acyclovir (98.0%, TCI America) (acyclovir), citric acid (anhydrous, >99.5%, Alfa Aesar), sodium hypophosphite hydrate (SHP, Sigma-Aldrich), acetic acid (Glacial, GR, ACS, Merck), cellulose acetate (39.8 WT % acetyl, Sigma-Aldrich), dichloromethane (for analysis EMSURE, Sigma-Aldrich), methanol (\geq 99.8% (GC), Sigma-Aldrich), dimethyl sulfoxide (DMSO, >99.9%, Sigma-Aldrich), phosphate-buffered saline tablets (Sigma-Aldrich), and sodium acetate (anhydrous, ACS, 99%, Alfa Aesar) were used without further purification. The high-quality water was distilled using a Millipore Milli-Q ultrapure water system (Millipore, USA)

2.2. Generation of Cross-Linked HP β CD/Acyclovir Inclusion Complex Nanofibers. First, a clear solution of HP β CD was prepared in distilled water having 180% (w/v) solid concentration. Afterward, acyclovir was added to the aqueous solution of HP β CD to provide a 2:1 (CD/drug) molar ratio (corresponding to ~5%, w/w with respect to total sample amount) and stirred overnight at room temperature to obtain an inclusion complex (IC). Then, the cross-linker (citric acid, 30% (w/w, according to HP β CD concentration)) and the initiator (SHP, 2% (w/w, according to HP β CD concentration)) were added to the HP β CD/acyclovir-IC solution and stirred until citric acid and SHP

completely dissolved. The pristine HP β CD (180% (w/v)) solution and $HP\beta CD$ solution (180% (w/v)) including the same ratio of citric acid (30%, w/w) and SHP (2%, w/w) were prepared in water as well. As a control, the solutions of pristine cellulose acetate (CA) (12%, w/v) and CA (12%, w/v)/acyclovir (~5%, w/w) were also prepared in a dichloromethane/methanol (4:1, v/v) blend system. The electrospinning equipment (Spingenix, model: SG100, Palo Alto, USA) was used to generate nanofibers. For this, the prepared solution was separately loaded in plastic disposable syringes attached with the metallic nozzle (21-23 G) and fed through this nozzle with a flow rate of 0.3-0.5 mL/h. The high voltage (15-17 kV) was applied to the nozzle for the formation and deposition of nanofibers on the fixed metal collector (15 cm away from the nozzle). The free-standing nanofibrous layers were efficiently obtained at ambient conditions recorded to be 19 °C with a relative humidity of 45%. For the cross-linking process, the $HP\beta CD/acyclovir-IC$ and $HP\beta CD$ nanofibers, which were mixed with cross-linker/initiator systems, were thermally treated at 175 °C for 1 h in an oven open to air.

2.3. Morphological Analysis of Nanofibers. The morphology of the samples was determined using a scanning electron microscope (SEM, Tescan MIRA3, Czech Republic). Prior to the measurements, samples were sputtered with a thin layer of Au/Pd to remove the charging problem. The average diameter (AD) of nanofibers ($n = \sim 100$) was validated by ImageJ software and provided as the average diameter \pm standard deviation.

2.4. Structural Characterization. Attenuated total reflectance Fourier transform infrared (ATR-FTIR) spectrometry (PerkinElmer, USA) was used for recording the Fourier transform infrared (FTIR) spectra of the samples. Each spectrum was taken in the range of 4000-600 cm⁻¹ upon 32 scans at a resolution of 4 cm⁻¹. A thermogravimetric analyzer (TGA, Q500, TA Instruments, USA) was used for examining the thermal profile of the samples. The heating rate of 20 °C/min was applied to increase the temperature from room temperature to 600 °C (N₂). The thermal profile of the samples was also verified by using a differential scanning calorimeter (DSC, Q2000, TA Instruments, USA). The samples put in the Tzero aluminum pan were heated by employing the heating rate of 10 °C/min from 0 to 280 °C (N2). The X-ray diffraction patterns of the samples were determined by an X-ray diffractometer (XRD, Bruker D8 Advance ECO). The XRD graphs were recorded in the range of $2\Theta = 5^{\circ} - 30^{\circ}$ by $Cu - K\alpha$ radiation (40 kV) and 25 mA).

2.5. Dissolution and Swelling Tests. For the water dissolution profile, pristine HP β CD nanofibers and HP β CD and HP β CD/acyclovir-IC nanofibers including cross-linker systems (thermally treated and not treated), having ~5 mg of weight, were placed into vials, and then 5 mL of distilled water was poured onto the samples. Videos were recorded at the same time to follow the dissolution behavior of the samples (Videos S1–S2). The swelling profiles of cross-linked HP β CD nanofibers and CA were examined using the two different aqueous systems of PBS buffer (pH 7.4) and acetate buffer (pH 5.4). First, ~1 mg of nanofibers was immersed in 1 mL of buffer solution and shaken on the incubator shaker for 24 h at 37 °C. Then, swollen samples were removed from the liquid mediums and weighed using an analytic balance after removing the excess amount of liquid medium from the samples. The swelling ratio (%) was calculated using the following formula

Swelling ratio (%) =
$$(W - W_0)/W_0 \times 100$$
 (F1)

where W and W_0 are the weights of the swollen and initial nanofibers, respectively.

2.6. Loading Efficiency Test. To determine the loading efficiency of non-cross-linked HP β CD/acyclovir-IC and CA/acyclovir nanofibers, ~10 mg of samples was completely dissolved in dimethyl sulfoxide (DMSO) (5 mL). The loading efficiency value of the samples was verified by UV-vis measurements (PerkinElmer, Lambda 35, USA) (251 nm). The calibration curve of acyclovir in DMSO showed acceptability with $R^2 \geq 0.99$. Three replications were performed for each sample, and the results were provided as mean values \pm standard deviations. The following formula was used to calculate the loading efficiency (%).

ACS Applied Bio Materials www.acsabm.org Article

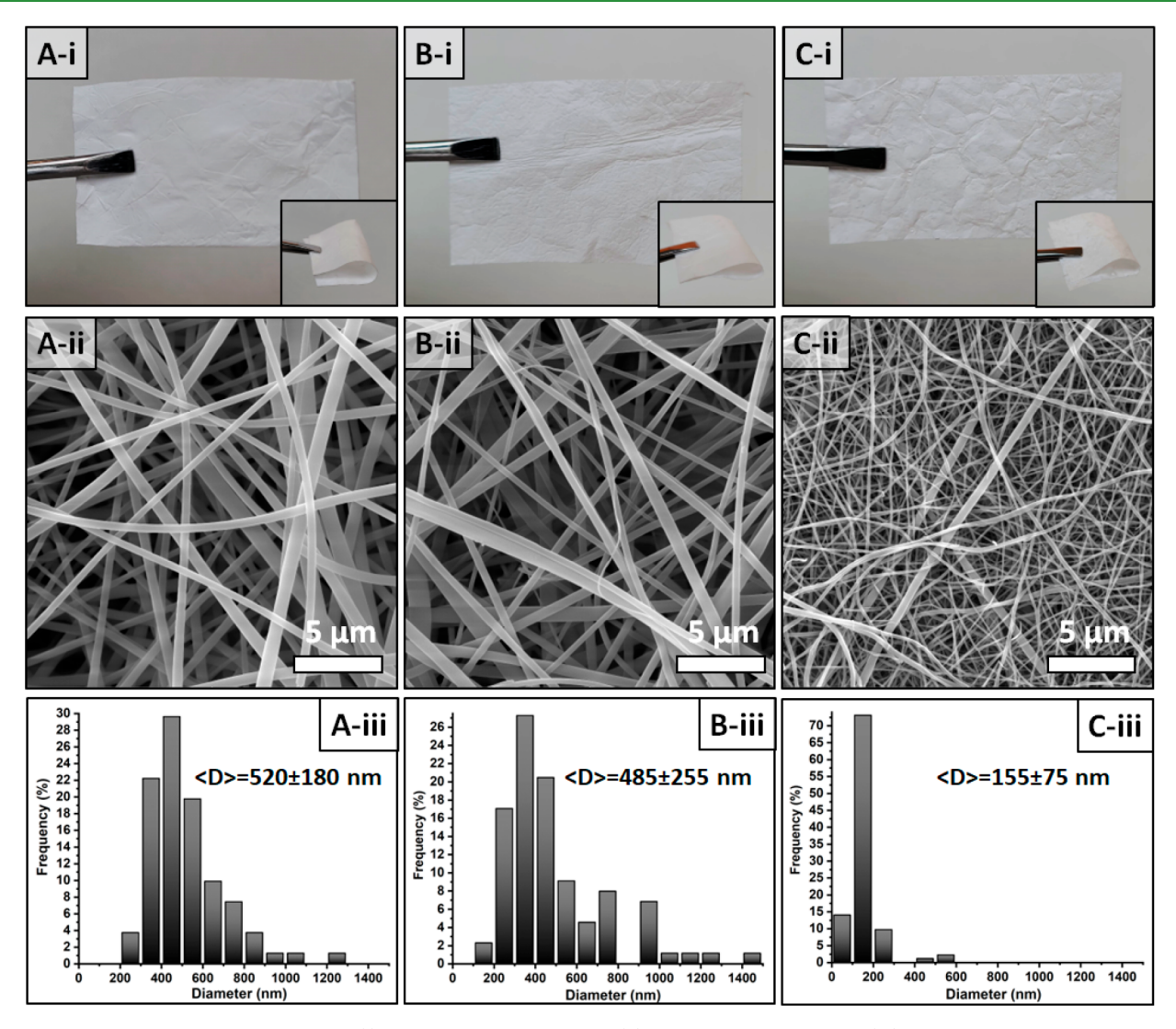


Figure 2. Morphological findings. The photos (i), representative SEM images (ii), and fiber size distribution (iii) of ultimate electrospun nanofibers of (A) pristine HP β CD, (B) cross-linked HP β CD, and (C) cross-linked HP β CD/acyclovir-IC.

Loading efficiency (%) =
$$Ce/Ct \times 100$$
 (F2)

where Ce and Ct are the concentration of loaded acyclovir and the initial concentration of acyclovir, respectively.

2.7. In Vitro Release Test. The time-dependent release test of cross-linked HP β CD/acyclovir-IC and CA/acyclovir nanofibers was conducted in two different liquid media having pH values of 7.4 and 5.5. For this, ~10 mg of sample was immersed in 10 mL of buffer systems (37 °C) and shaken on the incubator shaker at 150 rpm at predetermined time intervals, and 0.75 mL of aliquot was withdrawn. Fresh aliquot was re-added to the systems. The UV-vis spectroscopy measurements (250 nm) were performed to determine the released acyclovir amount from nanofibers. The calibration curve of acyclovir in buffer solutions showed $R^2 \ge 0.99$ linearity, and the released amount of acyclovir was calculated by converting the absorbance intensity of aliquots into concentration %. Triplicate tests were carried out for each sample (mean values \pm standard deviations), and release kinetics were examined by using different kinetic models (see Supporting Information).

2.8. Statistical Analyses. The statistical analyses were performed using the one-way/two-way variance (ANOVA). OriginLab (Origin 2023, USA) was used for all of these ANOVA analyses. A Tukey comparison test was applied to follow the significant difference between samples (p < 0.05).

3. RESULTS AND DISCUSSION

3.1. Morphology of Electrospun Nanofibers. As it has been reported in our previous study, the HP β CD/acyclovir-IC system having a 2:1 molar ratio (CD/drug) enables us to obtain free-standing nanofibers successfully. 42 Therefore, cross-linked $HP\beta CD/acyclovir-IC$ nanofibers have also been generated using the same molar ratio of 2:1 (CD/drug). Here, the acyclovir content of inclusion complex nanofibers was \sim 5% (w/w). The control sample of CA/acyclovir nanofibers was consequently generated with the same amount of acyclovir content (~5% (w/ w)). For the electrospinning of CA/acyclovir nanofibers, the solvent blend system of dichloromethane/methanol (4:1, v/v) was used differently from the aqueous system used in the case of $HP\beta CD/acyclovir-IC$ nanofibers. As control samples, pristine $HP\beta CD$, pristine CA, and acyclovir-free cross-linked $HP\beta CD$ nanofibers were electrospun, as well. It is noteworthy to mention that the polyCD-based nanofibers might be anticipated to be fragile due to the cross-linked network assembly of the small molecules of CD, differently from the chain structure of polymers. Nevertheless, the cross-linked HP β CD and HP β CD/ acyclovir-IC nanofibers were free-standing, with reasonable flexibility and mechanical integrity (Figure 2B,C-i) just like

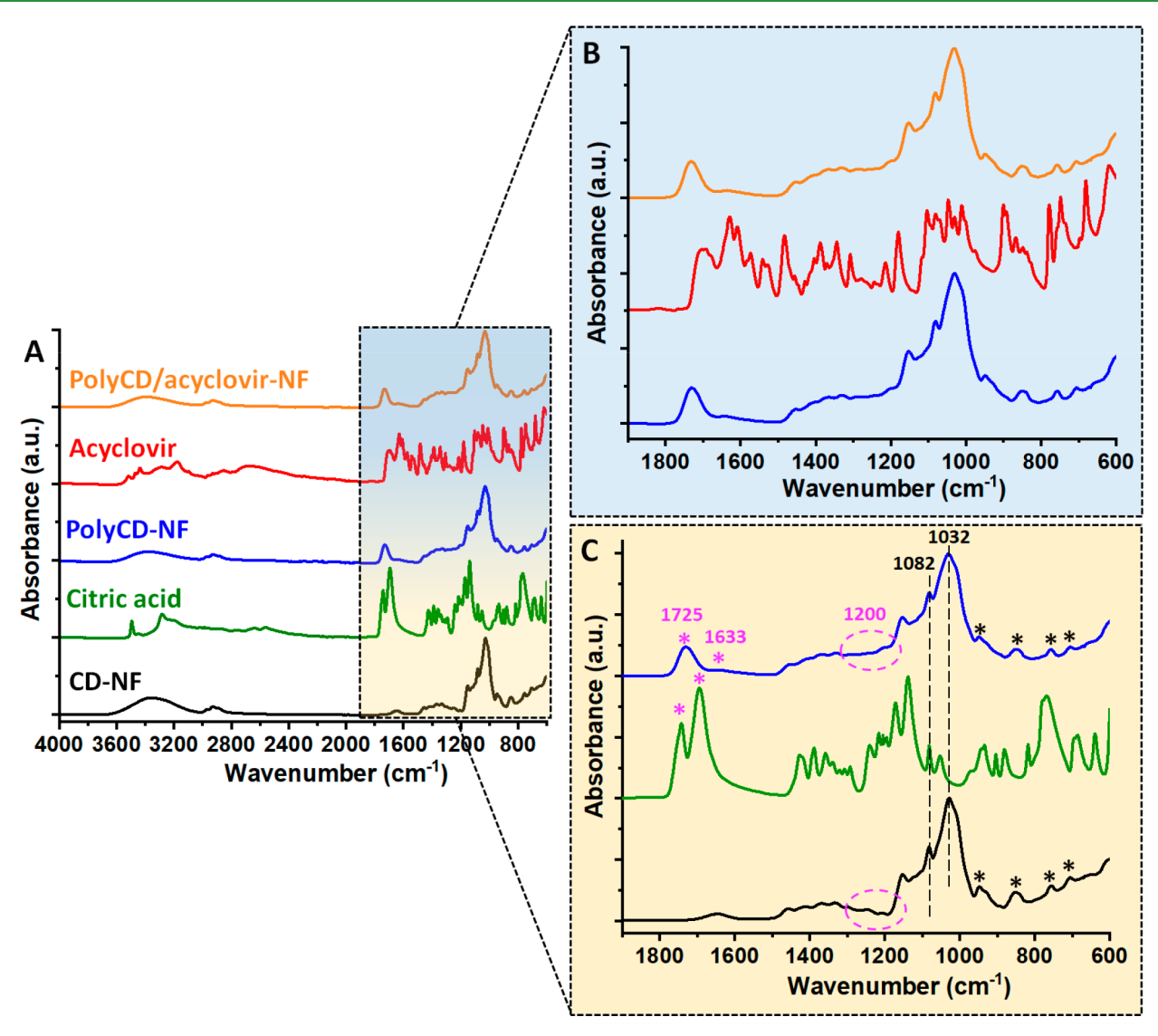


Figure 3. Chemical structure analysis. (A) The full and (B and C) expanded FTIR spectra of powder citric acid and acyclovir, pristine HP β CD nanofibers (CD-NF), cross-linked HP β CD nanofibers (PolyCD-NF) and cross-linked HP β CD/acyclovir-IC nanofibers (PolyCD/acyclovir-NF).

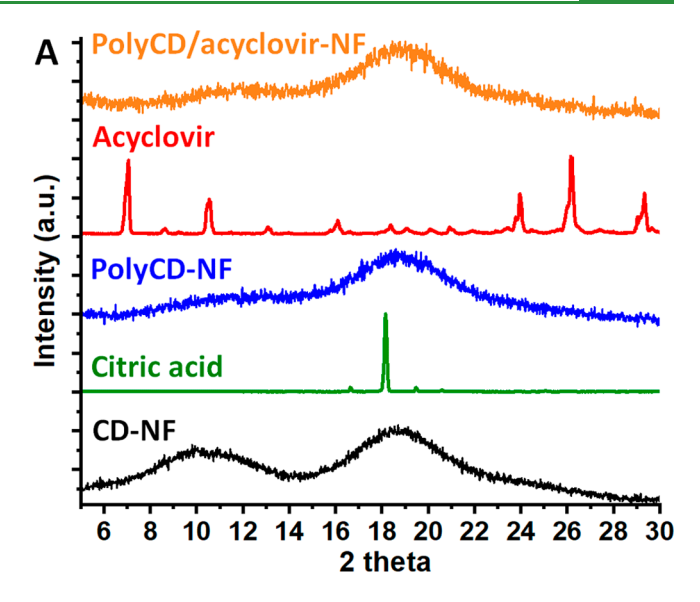
pristine HP β CD nanofibers (Figure 2A-i) and CA-based polymeric nanofibers (Figure S1). Moreover, there were no differences detected in the mechanical integrity of nanofibers before and after the cross-linking process. Figure 2 also indicates the SEM images (Figure 2A,B,C-ii) and the fiber size distribution graphs (Figure 2A,B,C-iii) of the same samples. It is obvious that the homogeneous and bead-free nanofibers were formed with a smooth surface texture. The average diameters (ADs) of pristine HP β CD, cross-linked HP β CD, and crosslinked HP β CD/acyclovir-IC nanofibers were 520 \pm 180, 485 \pm 255, and 155 \pm 75 nm, respectively. The differences in the ADs of samples can be attributed to the solution properties of viscosity, conductivity, polarity, and/or surface tension. The control samples of CA (570 \pm 170 nm) and CA/acyclovir (620 ± 250 nm) nanofibers were also obtained with homogeneous morphology and free-standing features (Figure S1).

3.2. Structural Characterization. FTIR analysis revealed the cross-linking process in the HP β CD nanofibers following thermal treatment. Figure 3 indicates the full and expanded FTIR spectra of samples. The presence of the prominent additional peak corresponding to the C=O stretching vibration of the ester moiety at around 1725 cm⁻¹ exhibited the cross-

linker being in the samples, while the pristine HP β CD-based sample did not indicate any absorption band in this region (Figure 3C).⁴⁸ On the other hand, the -OH bending peak of citric acid at 1695 cm⁻¹ was also observed in the case of crosslinked HP β CD nanofibers along with a significant shift (1633 cm⁻¹) and attenuated intensity. The shifts detected in the absorption bands of carbonyl and hydroxyl groups of citric acid and the lower $I_{1725/1633}$ ratio compared to pure citric acid $(I_{1740/1695})$ were attributed to the formation of the cross-linked CD network.⁴⁹ The reduction in the ratio of $I_{1725/1633}$ was ascribed to cross-linking because it demonstrated the increasing number of free carboxyl groups and the decreasing number of -OH groups in the structure of citric acid as a result of ester linkage formation (Figure 3C).⁴⁹ The absorption band at around 1200 cm⁻¹ in thermally treated HP β CD nanofibers, which was absent in pristine HP β CD samples, was due to the C-O-C stretching vibration of the ester linkage that was formed by the reaction between hydroxyl groups of HP β CD and the carboxyl groups of citric acid (Figure 3C). 48,49 The distinct absorption peaks of HP β CD at around 1154, 1081, and 1028 cm⁻¹ were due to the stretching vibrations of the antisymmetric C-O-C glycosidic bridge and coupled C-C/C-O, so and the

other absorption bands including 947, 851, 755, and 705 cm⁻¹ were observed at the same wavelength with a similar pattern in cross-linked HP β CD nanofibers (Figure 3C). This suggested that the main structure of HP β CD was protected after thermal treatment. The increasing absorbance intensity ratio of I_{1081} / I_{1028} in cross-linked HP β CD nanofibers can also be attributed to the cross-link formation between citric acid and HP β CD. ^{38,51} For cross-linked HP β CD/acyclovir-IC nanofibers, the characteristic peaks of acyclovir were hindered by the absorption bands of HP β CD (Figure 3B). Thus, the FTIR spectrum of crosslinked HP β CD/acyclovir-IC nanofibers showed the same profile with cross-linked HP β CD nanofibers as a result of IC formation between CD and the drug molecule (Figure 3B).⁵² On the other hand, the physical mixture of drug and polymer in CA/acyclovir nanofibers led to an increase in the absorption intensity at different regions of the FTIR spectrum where acyclovir peaks existed prominently (Figure S2).

The effect of cross-linking on HP β CD-based systems and the physical state of components in the samples were further examined through XRD and DSC analyses (Figure 4). The hydroxy-propylated derivates of β CD showed an amorph XRD pattern having two broad peaks at around 10.3° and 18.6° (Figure 4A). 32 Accordingly, there was no melting point detected in the DSC thermogram of the pure HP β CD nanofibers (Figure 4B). However, an endothermic peak was observed at around \sim 76 °C related to water loss (Figure 4B). In the case of crosslinked HP β CD nanofibers, the crystalline peak (7.1°) and the melting point (156 °C) of citric were not detected in the XRD graph (Figure 4A) and DSC thermogram (Figure 4B), respectively, since it was homogeneously dissolved in electrospinning solution and then made to interact with CD through the cross-linking process. Moreover, cross-linked HP β CD nanofibers indicated one broad peak at 18.6°, differently from pure $HP\beta$ CD nanofibers, which might be due to the modified orientation of CD molecules as a result of the cross-linking process and/or shearing forces applied through electrospinning (Figure 4A). An additional endothermic peak (~260 °C) became apparent in the DSC thermogram of cross-linked $HP\beta CD$ nanofibers, and this can be assigned to a potential degradation within the structure of the CD network (Figure 4B). On the other hand, acyclovir has a crystal nature which can be clearly recognized by the distinct diffraction peaks (7.1°, 10.6°, 16.1°, 23.9°, 26.2°, and 29.4°) observed at the XRD graph (Figure 4A) and the melting point (258 °C) present at the DSC thermogram (Figure 4B). Acyclovir powder can be found in the different form of crystals, hydrated or unhydrated.⁵³ The XRD graph that was recorded confirmed the 3:2 acyclovir/H2O hydrated crystal type.⁵³ For cross-linked HPβCD/acyclovir nanofibers, identical XRD and DSC patterns were recorded with cross-linked HP β CD nanofibers in the absence of a crystal peak and the melting point of acyclovir (Figure 4A,B). This confirmed the complete encapsulation of the drug molecule into CD cavities which hindered the packing of acyclovir molecules into crystals during or after the electrospinning. On the other hand, the crystal peak and the melting point of acyclovir were, respectively, noticed in the XRD graph and DSC thermogram of CA/acyclovir nanofibers (Figure S3). This finding validated the dispersion of drug crystals in CA nanofibers without proper dissolving. It is noteworthy to mention that there was a difference detected at the XRD pattern and a shift at the melting point of acyclovir (252 °C) in the case of CA/acyclovir nanofibers (Figure S3). This result confirmed that CA could not protect the primary crystal state of acyclovir and caused a



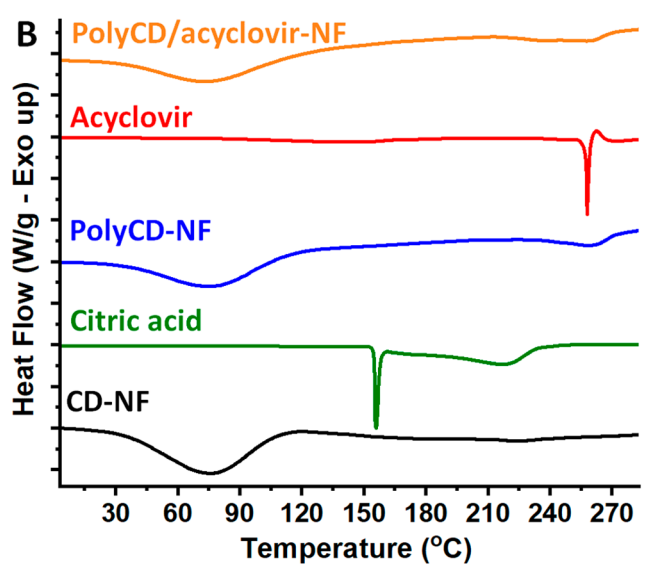


Figure 4. Crystal structural examination. (A) XRD patterns and (B) DSC thermograms of powder citric acid and acyclovir, pristine HP β CD nanofibers (CD-NF), cross-linked HP β CD nanofibers (PolyCD-NF), and cross-linked HP β CD/acyclovir-IC nanofibers (PolyCD/acyclovir-NF).

different hydrated crystal type of acyclovir having a 2:1 acyclovir/H₂O ratio. ⁵³

The thermal degradation profile of samples was examined using a thermal gravimetric analyzer (TGA) (Figure 5). For the TGA thermogram of cross-linked HP β CD nanofibers, the main thermal degradation step shifted to lower temperature (340 °C) compared to pristine HP β CD nanofibers (358 °C). This proved the existence of another type of connection between CD molecules in cross-linked samples differently from the noncross-linked CD matrix. An additional degradation step was also noticed at 267 °C for the cross-linked HP β CD nanofibers which can be attributed to the citric acid within the network structure. However, it was detected at the higher temperature compared to the main degradation of pure citric acid (195 °C) since it became a part of the cross-linked HP β CD network after the thermal treatment (Figure 5).³⁸ The respective degradation process was also discussed in the findings of DSC analyses in which an additional endothermic peak was observed at 260 °C

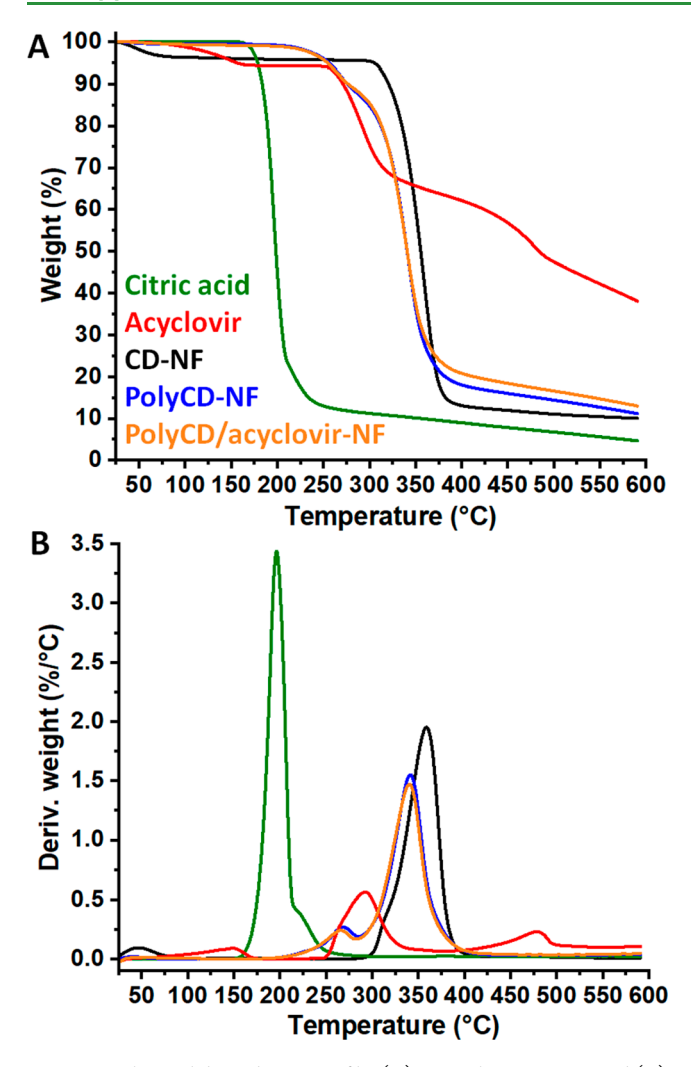


Figure 5. Thermal degradation profile. (A) TGA thermograms and (B) their derivative (DTG) of powder citric acid and acyclovir, pristine HP β CD nanofibers (CD-NF), cross-linked HP β CD nanofibers (PolyCD-NF) and cross-linked HP β CD/acyclovir-IC nanofibers (PolyCD/acyclovir-NF).

for cross-linked samples (Figure 4B). For acyclovir powder, we detected three steps of weight losses in the TGA thermogram. The initial step (max at ~150 °C) was observed owing to the water loss from the hydrated crystals of 3:2 acyclovir/H₂O.^{53,54} On the other hand, the hydroxyl ethoxy methyl side chain of acyclovir decayed from the purine unit at ~293 °C and degraded later on at ~478 °C, which was noticed as an additional two weight loss steps in the thermogram.^{53,55} In the case of crosslinked HP β CD/acyclovir-IC nanofibers, we obtained an identical thermogram with cross-linked HP β CD nanofibers (Figure 5). It is obvious that the acyclovir degradation was not identified as a distinct step in the TGA thermogram of crosslinked HP β CD/acyclovir-IC nanofibers. There was only a small decrease noticed at the main weight loss ratio (%) value of the derivative TGA thermogram (Figure 5B). These findings confirmed the incorporation of drug molecules into cross-linked $HP\beta CD/acyclovir-IC$ nanofibers along with an inclusion complex formation between the CD and drug. On the other hand, the TGA thermogram of pristine CA and CA/acyclovir nanofibers exhibited the main weight loss at 368 °C (Figure S4). Here, a small and separate degradation step was found at around 290 °C in the TGA thermogram of CA/acyclovir nanofibers

corresponding to the acyclovir degradation within the sample (Figure S4B). This demonstrated that the drug molecules were incorporated into the polymeric system in a way that facilitates physical mixing and without additional interaction.

3.3. Dissolution/Swelling and in Vitro Release Profile. The insolubility in water gained upon the thermal cross-linking procedure for HP β CD and HP β CD/acyclovir-IC nanofibers was confirmed by a dissolution test. Figure 6A shows the photos of test vials that were captured from Video S1 and Video S2. Here, the nanofibers of HP β CD and HP β CD/acyclovir-IC which included the cross-linker system but were not thermally treated rapidly dissolved upon contact with water just like pristine HP β CD nanofibers (Figure 6A). On the other hand, both nanofibers became insoluble in water after a thermal cross-linking procedure which was conducted at 175 °C for 1 h. The cross-linked HP β CD and HP β CD/acyclovir-IC nanofibers protected their fibrous structure even after being kept in water for 24 h as was shown in SEM images (Figure 6B,C).

One of the crucial features of wound dressing patches is the capacity for maintaining the body fluid, wound exudates, and metabolites. Therefore, a reasonable swelling property is expected from the wound care material which can also induce a moist microenvironment, boosting the wound healing progression. Depending on the hydrophilicity of the electrospinning carrier matrix, nanofibers can be a good candidate as wound dressing material owing to their high surface area and porous 3D structure which can provide actual penetration ways for liquid medium to be absorbed into the structure.² Therefore, the swelling profile of cross-linked HP β CD and CA nanofibers was examined in two different buffer media of PBS and acetate, having pH 7.4 and 5.4, respectively. Figure 7A represents the swelling ratio charts of samples. As it is seen, the swelling ratio of CA nanofibers showed a higher swelling ratio at pH 7.4 (1294 \pm 365%) compared to pH 5.4 (968 \pm 33%) after 24 h immersion, and this trend is in tune with the previous reports. The swelling ratio of cross-linked $HP\beta CD$ nanofibers was also found to be higher in PBS buffer (892 ± 63%) compared to acetate buffer (741 \pm 101%). The higher swelling ratio of cross-linked HP β CD nanofibers in pH 7.4 can be attributed to the negative COO groups in the structure which are formed by the deprotonation of carboxyl groups originating from the cross-linker. The anions (COO⁻) can repel each other to lead to the penetration of more water molecules into the cross-linked network. 59,60 Here, the detected swelling (water-uptake) ratio values (~740-890%) for the cross-linked $HP\beta CD$ -based nanofibers confirmed the hydrogel-forming features of these samples. As expected, acyclovir-incorporated samples displayed slightly lower swelling values compared to pristine cross-linked HP β CD and CA nanofibers (Figure 7A). Nevertheless, the meaningful swelling profile (~610-810%) observed for cross-linked HPβCD/acyclovir-IC nanofibers still suggested the acceptable efficiency of these nanofibrous hydrogels for the absorption of wound exudate during the treatments and ensured a moist environment for the wound area.⁶¹ Here, the loading efficiency test performed in DMSO showed that a huge amount of initial acyclovir content was protected during the process, and HP β CD/acyclovir-IC nanofibers were obtained with $89.6 \pm 9.2\%$ loading efficiency. On the other hand, CA/acyclovir nanofibers were produced with significantly lower loading efficiency (53.5 \pm 9.2%) compared to HP β CD/acyclovir-IC nanofibers (p < 0.05). Here, the better loading performance of HP β CD/acyclovir-IC nanofibers is due to encapsulation of acyclovir molecules into the HP β CD cavity

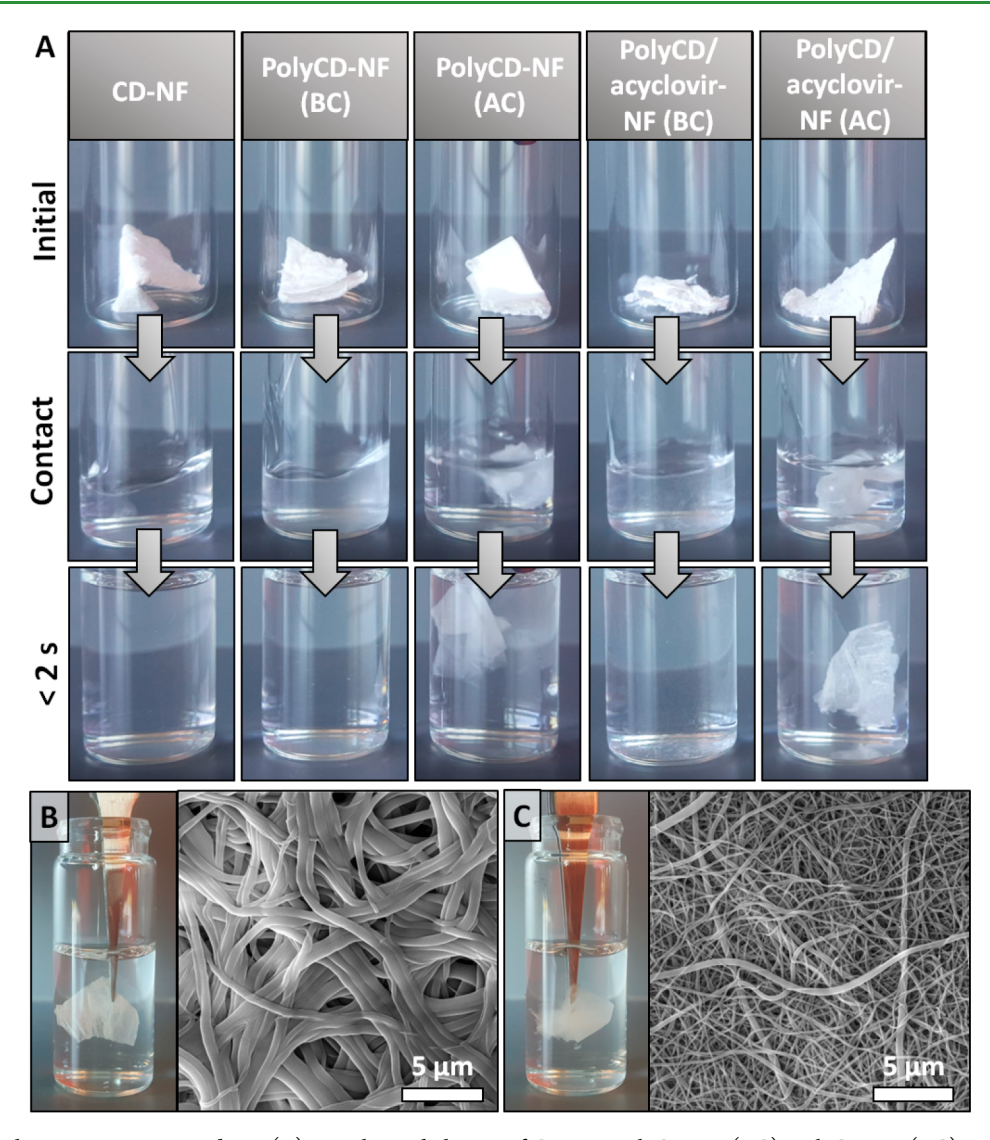


Figure 6. Sample behavior in aqueous medium. (A) Dissolution behavior of CD-NF, PolyCD-NF (BC), PolyCD-NF (AC), PolyCD/acyclovir-NF (BC), and PolyCD/acyclovir-NF (AC) (BC: before cross-link; AC: after cross-link). The photos and SEM images of (B) PolyCD-NF and (C) PolyCD/acyclovir-NF after being kept in water for 24 h.

by inclusion complexation. On the other hand, acyclovir was in crystal form in the CA-based system which might have limited the efficient participation of drug molecules in the electrospinning process, resulting in a lower loading efficiency. These findings are also consistent with XRD and DSC results where the amorphous and crystal distribution of drugs in HP β CD/acyclovir-IC and CA/acyclovir nanofibers was confirmed, respectively.

Figure 7B depicted the *in vitro* release profiles of cross-linked HP β CD/acyclovir-IC and CA/acyclovir nanofibers in the two different pH values of 7.4 and 5.4. Here, it is noteworthy to mention that any difference was detected between the UV absorption profile of cross-linked HP β CD/acyclovir-IC or CA/acyclovir nanofibers during the release test for both pH 7.4 and pH 5.4 buffers, and they were just like the UV spectrum of the pristine drug molecule (Figure S5). As seen for both pH systems, cross-linked HP β CD/acyclovir-IC nanofibers released a higher amount of drug molecules compared to CA/acyclovir nanofibers despite the higher swelling profile of CA-based systems. Additionally, HP β CD/acyclovir nanofibers, respectively, reached the released amount of 87.8 \pm 0.8% and 61.2 \pm 6.7%

at pH 7.4 and 5.4 in the first 30 min (Figure 7C) and then showed a steady profile up to 3 days (Figure 7B). Here, it is also noteworthy to mention that the formation of cross-linked CD nanofibrous hydrogels overcame the initial burst release of acyclovir. In the related study of Kazsoki et al., the core/shell nanofibers of PVA/PVP and hypromellose were used just to obtain this effect. 46 The control sample of CA/acyclovir nanofibers released just 7.2 \pm 1.4% and 7.6 \pm 0.7% of drug molecules at pH 7.4 and 5.4, respectively, in 30 min (Figure 7C) and reached the maximum released amount of $38.1 \pm 1.4\%$ and $29.3 \pm 4.9\%$ in 1-2 days (Figure 7B). In comparison with $HP\beta CD/acyclovir$ nanofibers, acyclovir existed in the crystal state in CA/acyclovir, which was also confirmed by XRD and DSC findings (Figure 4). Therefore, the release of drugs from CA/acyclovir nanofibers happened by the gradual dissolution of acyclovir crystals in the buffer mediums at progressing time intervals. On the other hand, the inclusion complex formation and interaction between acyclovir and HP β CD ensured an enhanced dissolution and release of drug molecules in the case of $HP\beta CD/acyclovir-IC$ nanofibers. 42

ACS Applied Bio Materials www.acsabm.org

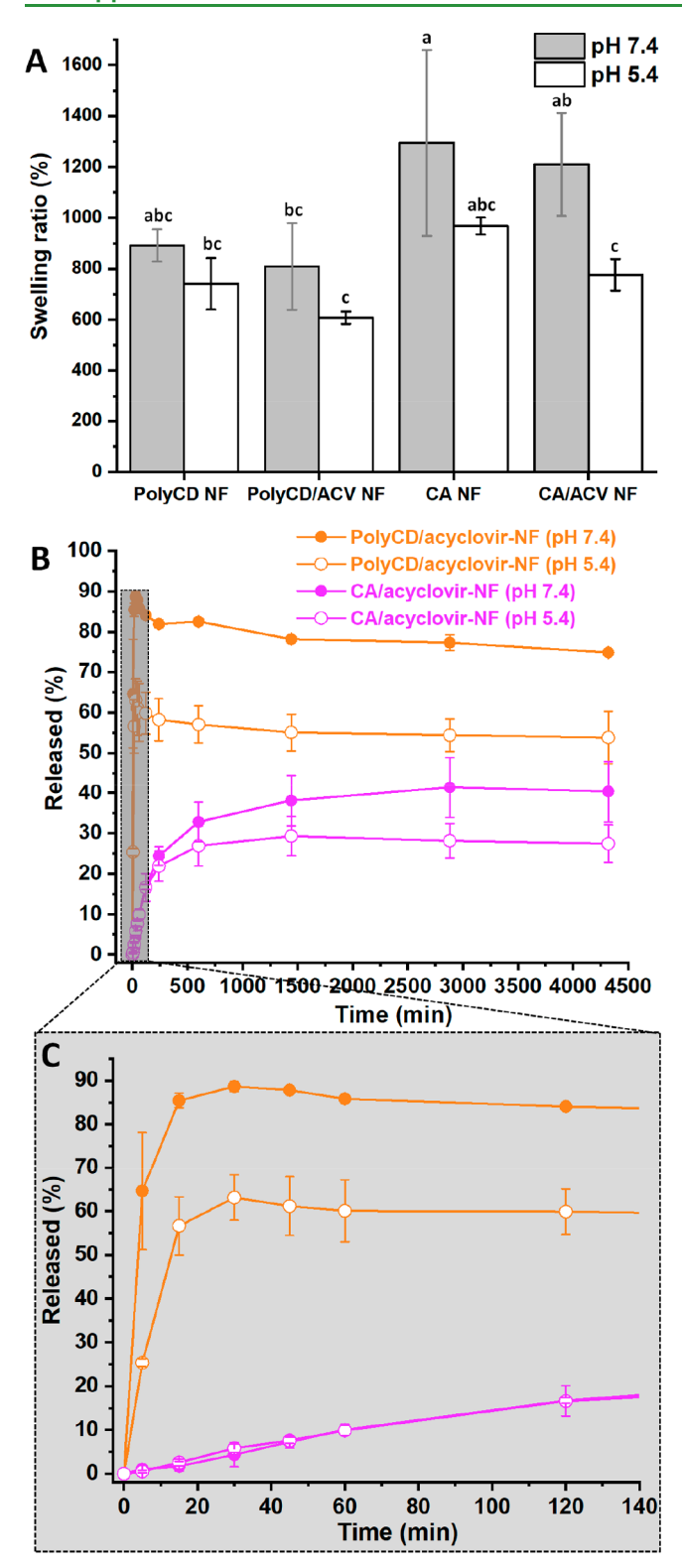


Figure 7. Results of swelling and release tests. (A) Swelling ratio and (B and C) time-dependent release profiles of HP β CD/acyclovir-IC nanofibers (PolyCD/acyclovir-NF) and CA/acyclovir nanofibers (CA/acyclovir-NF) in PBS (pH 7.4) and acetate (pH 5.4) buffers. (Mean swelling values that do not share a letter are significantly different (p < 0.05).)

In this study, the pH values of 5.4 and 7.4 were used for the *in vitro* release tests which, respectively, represent the approximate pH range in healthy skin and the wound area.⁶² Essentially,

acyclovir shows higher solubility at lower pH due to protonation of the drug molecules in aqueous medium.⁶³ However, it was detected that both cross-linked HP\(\beta CD/acyclovir \) and CA/ acyclovir nanofibers released a higher amount of drug in the pH 7.4 environment compared to that at pH 5.4 (Figure 7B). This can be ascribed to the higher swelling property of samples in the buffer medium of pH 7.4 than that of pH 5.4. It is noteworthy to mention that CA/acyclovir nanofibers started to show the release difference between these two pH values as of 2 h. On the other hand, cross-linked HP β CD/acyclovir nanofibers indicated a significant difference between pH 7.4 and 5.4 even in the first 5 min with release concentrations of 64.6 \pm 13.4% and 25.4 \pm 0.9%, respectively (Figure 7C). As was also confirmed by statistical analysis, cross-linked HP β CD/acyclovir nanofibers displayed a significant difference (p < 0.05) in terms of pHdependent release of the drug compound, whereas this difference was not statistically different for CA/acyclovir nanofibers (p > 0.05). Here, amorphous distribution and enhanced solubility of acyclovir by inclusion complexation with CD ensured the faster and more prominent pH-dependent release of drug from HPβCD/acyclovir nanofibrous hydrogel accordingly to the swelling behavior of this sample. Contrary to this, the acyclovir crystals gradually dissolved and diffused from CA/acyclovir nanofibers through the aqueous medium. Thus, we could not detect a difference, and CA samples released an identical amount of drug molecules in the first 2 h for both pH 5.4 and 7.4 based systems. Briefly, the enhanced release of acyclovir at pH 7.4 from cross-linked HPβCD/acyclovir-IC nanofibers and the acceptable swelling property might make this system favorable as a topical dosage formulation for wound treatments by ensuring the quick onset of action and the absorption of wound exudate during the administrations. It is noteworthy to mention that cross-linked HPβCD/acyclovir-IC nanofibrous hydrogels still kept their fibrous features by the end of the release test that was conducted for 3 days (Figure S6).

Article

The release profiles of samples were also fitted to different kinetic models in order to examine the release kinetics. The formulations and the correlation coefficient (R^2) values (Table S1) were summarized in Supporting Information. It was concluded from R^2 values that the release profile of cross-linked $HP\beta CD/acyclovir$ nanofibers was not compatible with the applied models of zero/first order kinetics and Higuchi and Korsmeyer-Peppas. On the other hand, the diffusion exponent (n) value of the Korsmeyer-Peppas model was found to be $n < \infty$ 0.45 (Table S1) for this sample, and this suggested the diffusionbased release of drug molecules from the carrier matrix (Fickian mechanism).⁶⁴ In our previous studies in which we reported the orally fast-disintegrating delivery systems from CD-IC nanofibers, we confirmed the non-time-dependent, non-Fickian diffusion and erosion-controlled release of active compounds using kinetic models. ^{33–35,42} In this study, we developed a crosslinked CD-IC nanofibrous system differently from our previous reports. Thus, we obtained a diffusion-based and rapid release profile for the drug molecule due to the undissolved feature of the film and the improved dissolution property of drug by inclusion complexation, respectively. Here, CA/acyclovir nanofibers indicated better fitting with the kinetic models compared to cross-linked HP β CD/acyclovir nanofibers (Table S1). It was noticed that CA/acyclovir nanofibers had a relatively higher consistency with the Korsmeyer-Peppas model among others (Table S1). Accordingly, the diffusion exponent (n) value was found in the 0.45 < n < 0.89 range, referring to the irregular and

non-Fickian diffusion release profile of acyclovir from CA/acyclovir nanofibers. ^{64,65}

4. CONCLUSION

Electrospinning offers a wide range of possibilities for the development of a variety of biomedical substrates, and wound healing dressing is one of the most favorably studied due to the similarity of electrospun nanofibrous materials to the extracellular matrix. In this study, it was aimed to generate a wound care material from the electrospun nanofibers of starch-derived natural cyclodextrin molecules in the form of free-standing and flexible nanofibers. For this purpose, highly water-soluble hydroxypropyl- β -cyclodextrin (HP β CD) and a well-known antiviral drug molecule of acyclovir were used for the formation of inclusion complexes (ICs), which constitute the main body of electrospun nanofibers. Since the HPβCD/acyclovir-IC nanofibers are soluble in water, a cross-linking system was added to the electrospinning solution. Here, the GRAS chemical of citric acid was chosen as the cross-linking agent. The $HP\beta CD/$ acyclovir-IC nanofibers were obtained with self-standing, flexible features and with uniform fiber morphology. Afterward, these nanofibers were thermally treated (175 °C, 1 h) for the cross-linking process, and the insoluble sample was obtained, keeping its initial mechanical integration and fibrous structure. The ultimate $HP\beta CD/acyclovir-IC$ nanofiber was obtained with ~90% loading efficiency that corresponds to the ~4.5% acyclovir content. The structural analysis of FTIR, XRD, DSC, and TGA supported and proved the loading of drug molecules and inclusion complex formation between acyclovir and $HP\beta CD$ in the nanofibers and the cross-linking between the $HP\beta CD$ and citric acid molecules by the ester linkage. Besides the water stability, the cross-linked HP β CD/acyclovir-IC nanofibers also showed a hydrogel-forming feature with a reasonable swelling ratio (water uptake) in the range of ~610-810%. Therefore, due to its high water uptake property, cellulose acetate, which is one of the most commonly used biopolymers, was chosen to generate control nanofibrous samples (swelling ratio: $\sim 780-1210\%$). Here, the time-dependent *in vitro* release test was performed in two different buffer solutions which represent the microenvironments of wound (pH 7.4) and normal skin (pH 5.4). Cross-linked HP β CD/acyclovir-IC nanofibrous hydrogels displayed a significantly higher release % at pH 7.4 buffer than at pH 5.4, which can be considered advantageous for wound treatment from the point of pHdependent release potential. Additionally, HP β CD/acyclovir-IC nanofibers showed a better release profile compared to CA/ acyclovir nanofibers along with a higher release amount due to the enhanced solubility of acyclovir by inclusion complex formation with HP β CD. Briefly, using HP β CD as a carrier matrix during the electrospinning provided several advantages compared to the polymeric matrix. First of all, the electrospinning solution was prepared in water including the FDAapproved citric acid (GRAS) as the cross-linking agent in the absence of toxic organic solvents or chemicals. Second, the inclusion complexation capability of CD enabled the generation of nanofibers by loading a drug molecule without disrupting the fiber formation and by guaranteeing an improved aqueous solubility for the drug. Since acyclovir is an effective antiviral drug against the herpes simplex virus (HSV-1/2) and varicella zoster, the cross-linked $HP\beta CD/acyclovir-IC$ nanofibrous hydrogels can be a promising alternative to the commercial dosage forms of acyclovir (Zovirax cream or Compeed Cold Sore Patch) as a wound healing patch which can be applied for

the topical treatment of cold sores, zoster, and chicken pox wound spots. Here, the acceptable swelling property of nanofibrous hydrogels can ensure the maintenance of wound exudates and induce the moist microenvironment. Here, the self-standing and flexible features of electrospun nanofibers, which make the folding and handling of samples easy, can also enable the integration of these materials with another biomedical substance depending on the application's purposes. To conclude, the cross-linked CD inclusion complex nanofibrous hydrogels might hold high potential as a novel wound healing dressing, and this "green" approach can be extended for further and different biomedical applications depending on the desired active ingredients. Here, the inclusion complex formation capability of CD molecules with numerous types of active agents would be evidence of the applicability of this approach for different drug molecules and therapeutic purposes.

ASSOCIATED CONTENT

5 Supporting Information

The Supporting Information is available free of charge at https://pubs.acs.org/doi/10.1021/acsabm.3c00446.

SEM images, FTIR and XRD spectra, and DSC and TGA thermograms of CA/acyclovir nanofibers; the representative UV spectra recorded during the release test for crosslinked HP β CD/acyclovir and CA/acyclovir nanofibers; SEM images of cross-linked HP β CD/acyclovir nanofibers after a release test; and kinetic calculations for release test (PDF)

Dissolution behavior of HP β CD-based nanofibers (MP4) Dissolution behavior of HP β CD/acyclovir-IC-based nanofibers before and after the cross-linking process (MP4)

AUTHOR INFORMATION

Corresponding Authors

Tamer Uyar — Fiber Science Program, Department of Human Centered Design College of Human Ecology, Cornell University, Ithaca, New York 14853, United States; orcid.org/0000-0002-3989-4481; Email: tu46@cornell.edu

Asli Celebioglu — Fiber Science Program, Department of Human Centered Design College of Human Ecology, Cornell University, Ithaca, New York 14853, United States;
orcid.org/0000-0002-5563-5746; Email: ac2873@cornell.edu

Complete contact information is available at: https://pubs.acs.org/10.1021/acsabm.3c00446

Author Contributions

A.C. performed the conceptualization, methodology, investigation, and writing of the original draft. T.U. supervised the study and participated in conceptualization, methodology, editing the final version, funding acquisition, and project administration of the study.

Notes

The authors declare no competing financial interest.

ACKNOWLEDGMENTS

This work made use of the Cornell Center for Materials Research Shared Facilities which are supported through the NSF MRSEC program (DMR-1719875) and Department of Human Centered Design facilities.

REFERENCES

- (1) Kalva, S. N.; Augustine, R.; Al Mamun, A.; Dalvi, Y. B.; Vijay, N.; Hasan, A. Active Agents Loaded Extracellular Matrix Mimetic Electrospun Membranes for Wound Healing Applications. *J. Drug Delivery Sci. Technol.* **2021**, *63*, 102500.
- (2) Gao, C.; Zhang, L.; Wang, J.; Jin, M.; Tang, Q.; Chen, Z.; Cheng, Y.; Yang, R.; Zhao, G. Electrospun Nanofibers Promote Wound Healing: Theories, Techniques, and Perspectives. *J. Mater. Chem. B* **2021**, *9*, 3106–3130.
- (3) Memic, A.; Abdullah, T.; Mohammed, H. S.; Joshi Navare, K.; Colombani, T.; Bencherif, S. A. Latest Progress in Electrospun Nanofibers for Wound Healing Applications. *ACS Appl. Bio Mater.* **2019**, *2*, 952–969.
- (4) Singh, S.; Young, A.; McNaught, C.-E. The Physiology of Wound Healing. Surg. 2017, 35, 473–477.
- (5) Sethuram, L.; Thomas, J. Therapeutic Applications of Electrospun Nanofibers Impregnated with Various Biological Macromolecules for Effective Wound Healing Strategy-A Review. *Biomed. Pharmacother.* **2023**, *157*, 113996.
- (6) Dong, Y.; Zheng, Y.; Zhang, K.; Yao, Y.; Wang, L.; Li, X.; Yu, J.; Ding, B. Electrospun Nanofibrous Materials for Wound Healing. *Adv. Fiber Mater.* **2020**, *2*, 212–227.
- (7) Golba, B.; Kalaoglu-Altan, O. I.; Sanyal, R.; Sanyal, A. Hydrophilic Cross-Linked Polymeric Nanofibers Using Electrospinning: Imparting Aqueous Stability to Enable Biomedical Applications. *ACS Appl. Polym. Mater.* **2022**, *4*, 1–17.
- (8) Xue, J.; Wu, T.; Dai, Y.; Xia, Y. Electrospinning and Electrospun Nanofibers: Methods, Materials, and Applications. *Chem. Rev.* **2019**, 119, 5298–5415.
- (9) Si, Y.; Shi, S.; Hu, J. Applications of Electrospinning in Human Health: From Detection, Protection, Regulation to Reconstruction. *Nano Today* **2023**, *48*, 101723.
- (10) Moholkar, D. N.; Sadalage, P. S.; Peixoto, D.; Paiva-Santos, A. C.; Pawar, K. D. Recent Advances in Biopolymer-Based Formulations for Wound Healing Applications. *Eur. Polym. J.* **2021**, *160*, 110784.
- (11) Leung, C. M.; Dhand, C.; Mayandi, V.; Ramalingam, R.; Lim, F. P.; Barathi, V. A.; Dwivedi, N.; Orive, G.; Beuerman, R. W.; Ramakrishna, S.; et al. Wound Healing Properties of Magnesium Mineralized Antimicrobial Nanofibre Dressings Containing Chondroitin Sulphate-a Comparison between Blend and Core-Shell Nanofibres. *Biomater. Sci.* 2020, 8, 3454–3471.
- (12) Amiri, N.; Ajami, S.; Shahroodi, A.; Jannatabadi, N.; Darban, S. A.; Bazzaz, B. S. F.; Pishavar, E.; Kalalinia, F.; Movaffagh, J. Teicoplanin-Loaded Chitosan-PEO Nanofibers for Local Antibiotic Delivery and Wound Healing. *Int. J. Biol. Macromol.* **2020**, *162*, 645–656.
- (13) Cestari, M.; Caldas, B. S.; Fonseca, D. P.; Balbinot, R. B.; Lazarin-Bidóia, D.; Otsuka, I.; Nakamura, C. V.; Borsali, R.; Muniz, E. C. Silk Fibroin Nanofibers Containing Chondroitin Sulfate and Silver Sulfadiazine for Wound Healing Treatment. *J. Drug Delivery Sci. Technol.* **2022**, *70*, 103221.
- (14) Najafiasl, M.; Osfouri, S.; Azin, R.; Zaeri, S. Alginate-Based Electrospun Core/Shell Nanofibers Containing Dexpanthenol: A Good Candidate for Wound Dressing. *J. Drug Delivery Sci. Technol.* **2020**, *57*, 101708.
- (15) Ashraf, S. S.; Parivar, K.; Roodbari, N. H.; Mashayekhan, S.; Amini, N. Fabrication and Characterization of Biaxially Electrospun Collagen/Alginate Nanofibers, Improved with Rhodotorula Mucilaginosa Sp. GUMS16 Produced Exopolysaccharides for Wound Healing Applications. *Int. J. Biol. Macromol.* **2022**, *196*, 194–203.
- (16) Abdalkarim, S. Y. H.; Yu, H.-Y.; Wang, D.; Yao, J. Electrospun Poly (3-Hydroxybutyrate-Co-3-Hydroxy-Valerate)/Cellulose Reinforced Nanofibrous Membranes with ZnO Nanocrystals for Antibacterial Wound Dressings. *Cellulose* **2017**, *24*, 2925–2938.
- (17) Li, A.; Han, Z.; Li, Ž.; Li, J.; Li, X.; Zhang, Z. A PTHrP-2 Loaded Adhesive Cellulose Acetate Nanofiber Mat as Wound Dressing Accelerates Wound Healing. *Mater. Des.* **2021**, *212*, 110241.

- (18) Hussein, Y.; El-Fakharany, E. M.; Kamoun, E. A.; Loutfy, S. A.; Amin, R.; Taha, T. H.; Salim, S. A.; Amer, M. Electrospun PVA/ Hyaluronic Acid/L-Arginine Nanofibers for Wound Healing Applications: Nanofibers Optimization and in Vitro Bioevaluation. *Int. J. Biol. Macromol.* **2020**, *164*, 667–676.
- (19) Nejaddehbashi, F.; Hashemitabar, M.; Bayati, V.; Moghimipour, E.; Movaffagh, J.; Orazizadeh, M.; Abbaspour, M. Incorporation of Silver Sulfadiazine into an Electrospun Composite of Polycaprolactone as an Antibacterial Scaffold for Wound Healing in Rats. *Cell J.* **2020**, *21*, 379.
- (20) Cui, S.; Sun, X.; Li, K.; Gou, D.; Zhou, Y.; Hu, J.; Liu, Y. Polylactide Nanofibers Delivering Doxycycline for Chronic Wound Treatment. *Mater. Sci. Eng., C* **2019**, *104*, 109745.
- (21) Yu, M.; Huang, J.; Zhu, T.; Lu, J.; Liu, J.; Li, X.; Yan, X.; Liu, F. Liraglutide-Loaded PLGA/Gelatin Electrospun Nanofibrous Mats Promote Angiogenesis to Accelerate Diabetic Wound Healing via the Modulation of MiR-29b-3p. *Biomater. Sci.* **2020**, *8*, 4225–4238.
- (22) Kaniuk, L.; Berniak, K.; Lichawska-Cieslar, A.; Jura, J.; Karbowniczek, J. E.; Stachewicz, U. Accelerated Wound Closure Rate by Hyaluronic Acid Release from Coated PHBV Electrospun Fiber Scaffolds. J. Drug Delivery Sci. Technol. 2022, 77, 103855.
- (23) Liu, M.; Duan, X.-P.; Li, Y.-M.; Yang, D.-P.; Long, Y.-Z. Electrospun Nanofibers for Wound Healing. *Mater. Sci. Eng., C* **2017**, 76, 1413–1423.
- (24) Crini, G. A History of Cyclodextrins. Chem. Rev. 2014, 114, 10940-10975.
- (25) Jansook, P.; Ogawa, N.; Loftsson, T. Cyclodextrins: Structure, Physicochemical Properties and Pharmaceutical Applications. *Int. J. Pharm.* **2018**, 535, 272–284.
- (26) Braga, S. S. Cyclodextrin Superstructures for Drug Delivery. J. Drug Delivery Sci. Technol. 2022, 75, 103650.
- (27) Sharma, D.; Dhingra, S.; Banerjee, A.; Saha, S.; Bhattacharyya, J.; Satapathy, B. K. Designing Suture-Proof Cell-Attachable Copolymer-Mediated and Curcumin-β-Cyclodextrin Inclusion Complex Loaded Aliphatic Polyester-Based Electrospun Antibacterial Constructs. *Int. J. Biol. Macromol.* **2022**, 216, 397–413.
- (28) Xu, R.; Zhang, M.; Yao, J.; Wang, Y.; Ge, Y.; Kremenakova, D.; Militky, J.; Zhu, G. Highly Antibacterial Electrospun Double-Layer Mats for Preventing Secondary Wound Damage and Promoting Unidirectional Water Conduction in Wound Dressings. *J. Ind. Eng. Chem.* 2023, 119, 404–413.
- (29) Li, C.; Luo, X.; Li, L.; Cai, Y.; Kang, X.; Li, P. Carboxymethyl Chitosan-Based Electrospun Nanofibers with High Citral-Loading for Potential Anti-Infection Wound Dressings. *Int. J. Biol. Macromol.* **2022**, 209, 344–355.
- (30) Rajaram, R.; Lee, Y. R.; Angaiah, S. Supramolecular Assembly of Benzocaine Bearing Cyclodextrin Cavity via Host-Guest Complexes on Polyacrylonitrile as an Electrospun Nanofiber. *J. Pharm. Biomed. Anal.* **2023**, 225, 115223.
- (31) Séon-Lutz, M.; Couffin, A.-C.; Vignoud, S.; Schlatter, G.; Hébraud, A. Electrospinning in Water and in Situ Crosslinking of Hyaluronic Acid/Cyclodextrin Nanofibers: Towards Wound Dressing with Controlled Drug Release. *Carbohydr. Polym.* **2019**, 207, 276–287.
- (32) Celebioglu, A.; Uyar, T. Electrospinning of Nanofibers from Non-Polymeric Systems: Polymer-Free Nanofibers from Cyclodextrin Derivatives. *Nanoscale* **2012**, *4*, 621–631.
- (33) Celebioglu, A.; Tekant, D.; Kilic, M. E.; Durgun, E.; Uyar, T. Orally Fast-Disintegrating Resveratrol/Cyclodextrin Nanofibrous Films as a Potential Antioxidant Dietary Supplement. *ACS Food Sci. Technol.* **2022**, *2*, 568–580.
- (34) Hsiung, E.; Celebioglu, A.; Kilic, M. E.; Durgun, E.; Uyar, T. Ondansetron/Cyclodextrin Inclusion Complex Nanofibrous Webs for Potential Orally Fast-Disintegrating Antiemetic Drug Delivery. *Int. J. Pharm.* **2022**, *623*, 121921.
- (35) Celebioglu, A.; Wang, N.; Kilic, M. E.; Durgun, E.; Uyar, T. Orally Fast Disintegrating Cyclodextrin/Prednisolone Inclusion-Complex Nanofibrous Webs for Potential Steroid Medications. *Mol. Pharmaceutics* **2021**, *18*, 4486–4500.

- (36) Celebioglu, A.; Topuz, F.; Yildiz, Z. I.; Uyar, T. Efficient Removal of Polycyclic Aromatic Hydrocarbons and Heavy Metals from Water by Electrospun Nanofibrous Polycyclodextrin Membranes. *ACS Omega* **2019**, *4*, 7850–7860.
- (37) Celebioglu, A.; Topuz, F.; Uyar, T. Water-Insoluble Hydrophilic Electrospun Fibrous Mat of Cyclodextrin-Epichlorohydrin Polymer as Highly Effective Sorbent. *ACS Appl. Polym. Mater.* **2019**, *1*, 54–62.
- (38) Celebioglu, A.; Yildiz, Z. I.; Uyar, T. Electrospun Crosslinked Poly-Cyclodextrin Nanofibers: Highly Efficient Molecular Filtration Thru Host-Guest Inclusion Complexation. *Sci. Rep.* **2017**, *7*, 7369.
- (39) Cortesi, R.; Esposito, E. Acyclovir Delivery Systems. *Expert Opin. Drug Delivery* **2008**, *5*, 1217–1230.
- (40) Gurgel Assis, M. S.; Fernandes Pedrosa, T. C.; de Moraes, F. S.; Caldeira, T. G.; Pereira, G. R.; de Souza, J.; Ruela, A. L. M. Novel Insights to Enhance Therapeutics With Acyclovir in the Management of Herpes Simplex Encephalitis. *J. Pharm. Sci.* **2021**, *110*, 1557–1571.
- (41) Demirci, S.; Khiev, D.; Can, M.; Sahiner, M.; Biswal, M. R.; Ayyala, R. S.; Sahiner, N. Chemically Cross-Linked Poly (β -Cyclodextrin) Particles as Promising Drug Delivery Materials. *ACS Appl. Polym. Mater.* **2021**, *3*, 6238–6251.
- (42) Celebioglu, A.; Uyar, T. Electrospun Formulation of Acyclovir/Cyclodextrin Nanofibers for Fast-Dissolving Antiviral Drug Delivery. *Mater. Sci. Eng.*, C **2021**, *118*, 111514.
- (43) Aniagyei, S. E.; Sims, L. B.; Malik, D. A.; Tyo, K. M.; Curry, K. C.; Kim, W.; Hodge, D. A.; Duan, J.; Steinbach-Rankins, J. M. Evaluation of Poly (Lactic-Co-Glycolic Acid) and Poly (Dl-Lactide-Co-ε-Caprolactone) Electrospun Fibers for the Treatment of HSV-2 Infection. *Mater. Sci. Eng.*, C 2017, 72, 238–251.
- (44) Baskakova, A.; Awwad, S.; Jiménez, J. Q.; Gill, H.; Novikov, O.; Khaw, P. T.; Brocchini, S.; Zhilyakova, E.; Williams, G. R. Electrospun Formulations of Acyclovir, Ciprofloxacin and Cyanocobalamin for Ocular Drug Delivery. *Int. J. Pharm.* **2016**, *502*, 208–218.
- (45) Costa, T.; Ribeiro, A.; Machado, R.; Ribeiro, C.; Lanceros-Mendez, S.; Cavaco-Paulo, A. M.; Almeida, A.; das Neves, J.; Lúcio, M.; Viseu, T. Polymeric Electrospun Fibrous Dressings for Topical Co-Delivery of Acyclovir and Omega-3 Fatty Acids. *Front. Bioeng. Biotechnol.* **2019**, *7*, 390.
- (46) Kazsoki, A.; Palcsó, B.; Alpár, A.; Snoeck, R.; Andrei, G.; Zelkó, R. Formulation of Acyclovir (Core)-Dexpanthenol (Sheath) Nanofibrous Patches for the Treatment of Herpes Labialis. *Int. J. Pharm.* **2022**, *611*, 121354.
- (47) Salihu, R.; Abd Razak, S. I.; Ahmad Zawawi, N.; Rafiq Abdul Kadir, M.; Izzah Ismail, N.; Jusoh, N.; Riduan Mohamad, M.; Hasraf Mat Nayan, N. Citric Acid: A Green Cross-Linker of Biomaterials for Biomedical Applications. *Eur. Polym. J.* **2021**, *146*, 110271.
- (48) Zhao, D.; Zhao, L.; Zhu, C.; Tian, Z.; Shen, X. Synthesis and Properties of Water-Insoluble β -Cyclodextrin Polymer Crosslinked by Citric Acid with PEG-400 as Modifier. *Carbohydr. Polym.* **2009**, 78, 125–130.
- (49) Ghorpade, V. S.; Yadav, A. V.; Dias, R. J. Citric Acid Crosslinked Cyclodextrin/Hydroxypropylmethylcellulose Hydrogel Films for Hydrophobic Drug Delivery. *Int. J. Biol. Macromol.* **2016**, *93*, 75–86.
- (50) Yuan, C.; Liu, B.; Liu, H. Characterization of Hydroxypropyl-β-Cyclodextrins with Different Substitution Patterns via FTIR, GC-MS, and TG-DTA. *Carbohydr. Polym.* **2015**, *118*, 36–40.
- (51) Rodriguez-Tenreiro, C.; Alvarez-Lorenzo, C.; Rodriguez-Perez, A.; Concheiro, A.; Torres-Labandeira, J. J. New Cyclodextrin Hydrogels Cross-Linked with Diglycidylethers with a High Drug Loading and Controlled Release Ability. *Pharm. Res.* **2006**, 23, 121–130.
- (52) Mura, P. Analytical Techniques for Characterization of Cyclodextrin Complexes in the Solid State: A Review. *J. Pharm. Biomed. Anal.* **2015**, *113*, 226–238.
- (53) Lutker, K. M.; Quiñones, R.; Xu, J.; Ramamoorthy, A.; Matzger, A. J. Polymorphs and Hydrates of Acyclovir. *J. Pharm. Sci.* **2011**, *100*, 949–963
- (54) Sohn, Y. T.; Kim, S. H. Polymorphism and Pseudopolymorphism of Acyclovir. *Arch. Pharm. Res.* **2008**, *31*, 231–234.

- (55) Malik, N. S.; Ahmad, M.; Minhas, M. U. Cross-Linked β -Cyclodextrin and Carboxymethyl Cellulose Hydrogels for Controlled Drug Delivery of Acyclovir. *PLoS One* **2017**, *12*, No. e0172727.
- (56) Silvestre, A. J. D.; Freire, C. S. R.; Neto, C. P. Do Bacterial Cellulose Membranes Have Potential in Drug-Delivery Systems? *Expert Opin. Drug Delivery* **2014**, *11*, 1113–1124.
- (57) Bhandari, J.; Mishra, H.; Mishra, P. K.; Wimmer, R.; Ahmad, F. J.; Talegaonkar, S. Cellulose Nanofiber Aerogel as a Promising Biomaterial for Customized Oral Drug Delivery. *Int. J. Nanomedicine* **2017**, *12*, 2021.
- (58) Elmaghraby, N. A.; Omer, A. M.; Kenawy, E.-R.; Gaber, M.; El Nemr, A. Fabrication of Cellulose Acetate/Cellulose Nitrate/Carbon Black Nanofiber Composite for Oil Spill Treatment. *Biomass Convers. Biorefinery* **2022**, 1–19.
- (59) Gunathilake, T. M. S. U.; Ching, Y. C.; Chuah, C. H.; Abd Rahman, N.; Nai-Shang, L. PH-Responsive Poly (Lactic Acid)/Sodium Carboxymethyl Cellulose Film for Enhanced Delivery of Curcumin in Vitro. J. Drug Delivery Sci. Technol. 2020, 58, 101787.
- (60) Rana, J.; Goindi, G.; Kaur, N.; Sahu, O. Optimization and Synthesis of Cellulose Acetate Based Grafted Gel and Study of Swelling Characteristics. *Mater. Today Proc.* **2022**, *48*, 1614–1619.
- (61) Tungprapa, S.; Jangchud, I.; Supaphol, P. Release Characteristics of Four Model Drugs from Drug-Loaded Electrospun Cellulose Acetate Fiber Mats. *Polymer (Guildf)*. **2007**, *48*, 5030–5041.
- (62) Jiang, H.; Ochoa, M.; Waimin, J. F.; Rahimi, R.; Ziaie, B. A PH-Regulated Drug Delivery Dermal Patch for Targeting Infected Regions in Chronic Wounds. *Lab Chip* **2019**, *19*, 2265–2274.
- (63) Bencini, M.; Ranucci, E.; Ferruti, P.; Trotta, F.; Donalisio, M.; Cornaglia, M.; Lembo, D.; Cavalli, R. Preparation and in Vitro Evaluation of the Antiviral Activity of the Acyclovir Complex of a β -Cyclodextrin/Poly (Amidoamine) Copolymer. *J. Control. release* **2008**, 126, 17–25.
- (64) Peppas, N. A.; Narasimhan, B. Mathematical Models in Drug Delivery: How Modeling Has Shaped the Way We Design New Drug Delivery Systems. *I. Control. release* **2014**, *190*, 75–81.
- (65) Li, X.; Kanjwal, M. A.; Lin, L.; Chronakis, I. S. Electrospun Polyvinyl-Alcohol Nanofibers as Oral Fast-Dissolving Delivery System of Caffeine and Riboflavin. *Colloids Surf. B: Biointerfaces* **2013**, *103*, 182–188.